ICAS 2021 SHANG HAI
International Council of the Aeronautical Sciences
32nd Congress of the International Council of the Aeronautical Sciences
September 6-10, 2021
Pudong Shangri-La, Shanghai, China

STUDY ON CLOSED-LOOP CROSS COMPENSATION CONTROL TECHNOLOGY IN ACCELERATED FATIGUE TESTING

Hongwei Zhao[1, 2], Tao Han[1] , Zhenzhong Gu[3], Guangsheng Shi[4], Shihui Duan[1] & Jianmin Feng[1]

[1]Aircraft Strength Research Institute of China, [2]Xi'an jiaotong University, [3]Chongqing Hongyu Precision Industrial Co., Ltd., [4]Shenyang Aircraft Design & Research Institute of China

zhw_zhaohongwei@sina.com

Keywords: *Aircraft structure test; Closed-loop compensation control; Accelerated fatigue test; Multi-channel*

Abstract

A Aircraft structural fatigue test is a multi-component and multi-channel system, in which there are usually a large number of channels with significant interactions among them. Control is made more difficult because the tests are run in load control and the load cells usually move with the actuators. But fatigue test speed is limited mainly by this effect. To solve this problem, a closed-loop cross compensation control technique is proposed in this paper. Firstly, the Stiffness Coordinate Matrix (SCM) among the channels was deduced. Furthermore, the Cross Compensation Matrix (CCM) was derived by this matrix. Subsequently, CCM was introduced into the closed feedback control loop, and a cross compensation control algorithm was designed. Using that algorithm, the output signal of every channel was compensated crossly and adaptively in the aim to decrease the coupling effect among channels. At the same time, Hurwitz stability criterion was used to verify the stability of the new method. In order to validate the method in this paper, the technology using commercial off-the-shelf control techniques were implemented on a four channels full-scale fatigue testing system for wingbox structure of the MTS SYSTEMS. Results of the experiment showed that the method presented in this paper was efficient and reasonable to improve the efficiency of aircraft structure fatigue test, and could be widely used in relative test article. Some important findings may emerge from the future discussion and analysis.

1 Introduce

The structural fatigue test of aircraft structures plays an important role in the new aircraft development[1~6]. It is a crucial basis to predict structure life and a major mean to confirm critical parts of structure and its repairing cycle. Aircraft structural fatigue test is a multi-component and multi-channel system. In the process of test loading, deformation of loading points on test article differs greatly, thus the structure stiffness varied accordingly. Together with mechanical play between test article and loading system, there exists severe coupling phenomenon among loading control channels. Especially, the coupling becomes more effective with the increase of channel numbers[7~10]. The speed of fatigue test is limited mainly by this effect. To accelerate the fatigue test speed, load frequency should be increased, thus the test cycle would be cut down [11~12]. However, nature frequency of aircraft structure is very low

and the coupling effect among different channels stiffness is very strong, and this effect will be aggravated through the load frequency increase, and that will result in control precision depravation and test system unstability. Currently, it is difficult to relief that effect by the traditional Proportion-Integration-Differentiation(PID) controller which is used in current fatigue test system, so that the response speed of test system cannot be accelerated efficiently[13~14].

For fatigue test accelerated, most of researches focus on mainly loading spectrum simplifying[15~16]. A small quantity of study concerns test loading techniques[17~19]. But fatigue test accelerated also is studied from test controlling technology. In the early 1990s, Australia's Defense Science and Technology Organization (DSTO) proved the effectiveness of a number of advanced compensation techniques while creating a custom load control system for the International Follow-On Structural Test Project (IFOSTP) F/A-18 Empennage Fatigue Test. Developed to minimize test cycle and improve repeatability and loading accuracy, these combined techniques included non-linear gain scheduling, multi-channel feed-forward for cross coupling compensation, and non-linear load path compensation[20]. In 2005, Graeme Burnett in DSTO and Michael Sullivan from MTS System Corporation of USA developed an advanced control techniques for full-scale fatigue testing based on 1990s' research of DSTO. The study before ten years describes these performance-enhancing techniques and explores how DSTO is currently implementing these technology using commercial off-the-shelf control techniques on the 90 channels full-scale fatigue test of the BAE SYSTEMS Hawk Mk 127 aircraft[21]. The methods from DSTO are merely an open-loop compensation control scheme, so the test control accuracy cannot be compensated adaptively, not to decrease the coupling effect among loading channels effectively. Additionally, the fatigue test can be accelerated effectively using the technique in the test containing less loading points. However, because it is difficult to divide the cross coupling compensation matrix, the matrix orders is same as number of loading points, so that the order is higher and calculating time may be larger. So the technology cannot accelerate the fatigue test effectively in the fatigue test system which contains more controlling channels. To solve this problem, a closed-loop cross compensation control technique is developed in the paper based on the research of DSTO. Firstly, the closed-loop compensation control technique is introduced to single input single output (SISO) test system. And the stability of new method is proven by Hurwitz theory. Then the closed-loop cross coupling compensation control is discussed in the multi-channel fatigue test. Furthermore, Stiffness Coordinate Matrix (SCM) among controlling channels and the cross coupling compensation factor matrix is deduced. Finally, a wingbox structural fatigue test platform is designed to prove the new control method.

It is possible, with the use of closed-loop cross compensation control technique, to overcome these difficulties and improve system response and loading accuracy.

2 Single-Channel Control Technology

The analysis of a single channel controller is useful as it provides an adequate model to demonstrate closed-loop cross compensation control and describe new method needed to compensate output signal of controller or servo-valve response. The analysis within the paper does not include oil compressibility flow, leakage, cylinder friction, backlash, structural resonances or oil column resonances for simplification.

2.1 Closed-loop Compensated mechanism

Loading in aircraft structural fatigue test is

conducted actually by loading straight line which is main method in current test to approximates ideal loading curve, however, the error between line and curve is obvious, as shown in the Fig. 1. After a broken line is employed to approximate ideal cruve, as a result, the loading error decreases significantly. The compensated technique in the thesis is carried out by the broken line mode that a point in the ideal curve is marked and limited conditions is given. Detailed compensation technique will be discussed and analyzed afterward.

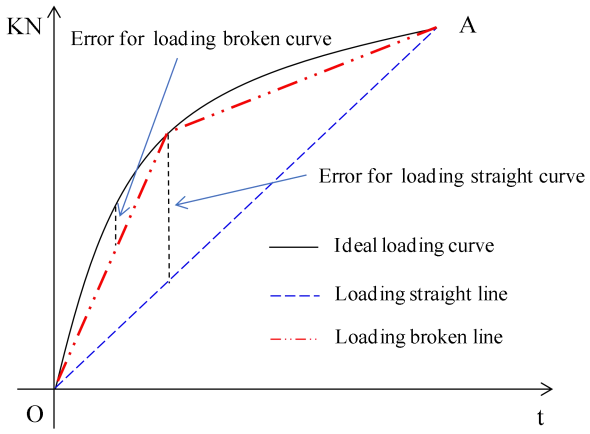

Fig. 1 Block diagram of closed-loop compensation controller

2.2 Single-channel control analysis

In Fig. 1, a traditional closed-loop control block diagram is drawn that has an input command, c, and an output that is the feedback control variable force, $G_1(s)$, $G_2(s)$, $G_3(s)$ and $G_4(s)$ are transfer function of PID controller, servo-valve, hydraulic actuator and test article respectively.

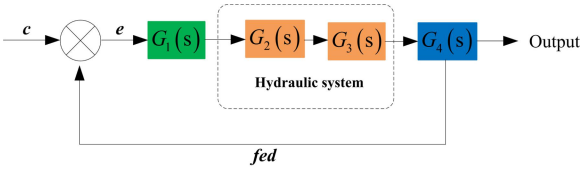

Fig. 2 Block diagram of traditional PID controller

This block diagram is interpreted as SISO test system. The variables, transfer function, block names from Figure 2 are used in a consistent manner throughout the paper. The structural test system consist out of PID controller, servo-valve, hydraulic actuator and structure (test article), where servo-valve and hydraulic actuator make up the hydraulic system. The test system is a closed-loop controlling system.

The transfer function of PID controller is described as Equation (1)..

$$G_1(s) = \frac{k_d s^2 + k_p s + k_i}{s} \tag{1}$$

Where, s is Laplace variable (all the transfer function in this paper are described by Laplace variable); k_P is proportion gain. k_i is integration gain. k_d is differentiation gain.

Because the test system may be vibrant with differentiation gain, PI controller is adapted to control testing loading. Equation (1) can be written as Equation (2)..

$$G_1(s) = \frac{k_p s + k_i}{s} \tag{2}$$

As Fig. 2 shown, PI controller can controls valve output signal which stay fixed during the test loading after tuned. During test loading, the test situation is influenced easily by outer factors, such as test article stiffness, hydraulic flow, pressure drop of oil pump and mechanical joints. The valve output signal may be attenuated in transferring process, so that the test system response and loading error cannot be controlled effectively. To solve this problem, a closed-loop compensation control technique is developed to improve loading controlling efficiency and system response.

2.3 Study of Single-channel compensation control

The valve output signal is compensated adaptively using inserting a compensated function between controller and controlled system, according to broken line mentioned, as Fig. 3 showed.

F(e), as a closed-loop compensation function, can

be described as Equation (3)..

$$F(e) = \begin{cases} (1+h) & (|e| \geq 1\%) \\ 1 (|e| < 1\%) \end{cases} \quad (3)$$

Where, e is control error; 1% is Empirical Value； h is compensation factor, boundary conditions of h is described using Equation (4).

$$1 \geq h \geq -1 \quad (4)$$

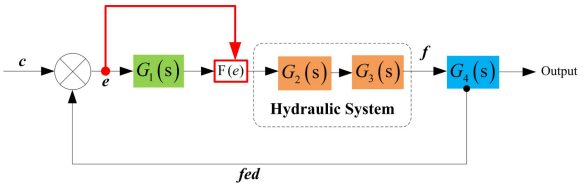

Fig. 3 Block diagram of closed-loop compensation controller

The transfer function of controller after compensated is interpreted by Equation (5).

$$G_1(s) = \frac{(1+h)\cdot k_p \cdot s + (1+h)\cdot k_i}{s} \quad (5)$$

The closed-loop compensation control in this paper can conduct compensation to valve output signal adaptively by controlling error. In fact, outer factors effect to system can be reflected to loading error. Theoretically, this closed-loop compensation control technology is same as valve output signal compensated in positive and negative directions, which can be equal to faculty of PI parameters, including improving system response and declining control error.

2.4 Stability provement on Closed-loop Compensation Control

The stability of closed-loop compensation system is discussed based on stability of initial test system. Hurwitz theory is used to prove the stability of closed-loop compensation system in this paper.

The open-loop transfer function of test system before compensated, G(s), is described as Equation (6).

$$\begin{aligned} G(s) &= G_1(s)G_2(s)G_3(s)G_4(s) \\ &= \frac{k_p s + k_i}{s} G_2(s)G_3(s)G_4(s) \end{aligned} \quad (6)$$

In literature[22], for transfer function of servo-valve, the denominator is second-order expression and contains constant term, while the numerator is 1; for transfer function of hydraulic actuator, the denominator is third-order expression and has no constant term, while the numerator is 1; as for transfer function of test article, the denominator and numerator are ninth-order expression and contain constant term. Therefore, Equation (6) can be confirmed as fifteenth-order. Furthermore, Equation (6) needs to be deduced as Equation (7).

$$G(s) = \frac{(k_p s + k_i)(b_0 s^9 + b_1 s^8 + \cdots + b_8 s + b_9)}{s(a_0 s^{14} + a_1 s^{13} + \cdots + a_{13} s + a_{14})} \quad (7)$$

Where, ai and bi are real number.

Equation (7) is expanded as Equation (8).

$$G(s) = \frac{\begin{array}{l} b_0 k_p s^{10} + (k_p b_1 + k_i b_0) s^9 + \\ (k_p b_2 + k_i b_1) s^8 + \cdots + \\ (k_p b_9 + k_i b_8) s + k_i b_9 \end{array}}{a_0 s^{15} + a_1 s^{14} + \cdots + a_{13} s^2 + a_{14} s} \quad (8)$$

The closed-loop Hurwitz characteristic equation can be described as Equation (9).

$$\begin{aligned} D(s) = {} & a_0 s^{15} + a_1 s^{14} + \cdots + a_4 s^{11} \\ & + (a_5 + b_0 k_p) s^{10} + (a_6 + k_p b_1 + k_i b_0) s^9 \\ & + (a_7 + k_p b_2 + k_i b_1) s^9 + \cdots \\ & + (a_{14} + k_p b_9 + k_i b_8) s + k_i b_9 \end{aligned} \quad (9)$$

Where, P and I gain exist in the coefficients between 1st and 10st term.

Assuming:

$$\begin{cases} c_i = a_i \ (0 \leq i \leq 4) \\ c_i = a_i + b_{i-5} k_p \ (i = 5) \\ c_i = a_i + b_{i-5} k_p + k_i b_{i-6} \ (6 \leq i \leq 14) \\ c_i = b_{i-6} k_i \ (i = 15) \end{cases} \quad (10)$$

Where, ci is real number. Equation (9) can be rewritten as Equation (11).

$$D(s) = c_0 s^{15} + c_1 s^{14} + \cdots + c_{14} s + c_{15} \quad (11)$$

Because the test system is stable before compensation, coefficients of Hurwitz characteristic equation is positive using Hurwitz theory, as Equation (12) shown.

$$c_i > 0 (1 \le i \le 15) \tag{12}$$

It can see from Equation (5) that the output signal of controller is amplified (1+h) times using control error judgment, and then Hurwitz Equation of test system is interpreted as Equation (13).

$$D'(s) = d_0 s^{15} + d_1 s^{14} + \cdots + d_{14} s + d_{15} \tag{13}$$

Where, di is real number, di can be described by Equation (14).

$$\begin{cases} d_i = c_i = a_i \left(0 \le i \le 4\right) \\ d_i = a_i + \left(1+h\right) \cdot b_{i-5} k_p \left(i = 5\right) \\ d_i = a_i + \left(1+h\right) \cdot b_{i-5} k_p \\ \quad + \left(1+h\right) \cdot k_i b_{i-6} \left(6 \le i \le 14\right) \\ d_i = \left(1+h\right) \cdot b_{i-6} k_i \left(i = 15\right) \end{cases} \tag{14}$$

It is easy to see that transfer function's order of all the test system is not changed from Equation (2), (5), (6) and (14). But coefficients of Hurwitz characteristic equation is changed partially from 6st term beginning. Combining Equation (4), Equation (15) can be obtained.

$$d_i > 0 (1 \le i \le 15) \tag{15}$$

After compensated, Hurwitz characteristic equation coefficients of closed-loop system are still positive. It should be noted that the new method has no impact on closed-loop stability.

3 Multi-Channel Compensation Control technology

3.1 Multi channel analysis

The analysis for a single-channel can be extended to multi-channel system with N channels. With reference to Fig. 2, for a multi-channel system: in place of a single command, c, and single feedback, f, there is an N term column vector command, [c], and an N term column vector feedback force, [f]. Block diagram of a simple two-channel closed-loop cross compensation control is shown in Fig. 3 to illustrate closed-loop cross compensation control between two channels. The closed-loop compensation control in this paper needs to be discussed in multi-channel fatigue test system to speed up fatigue test.

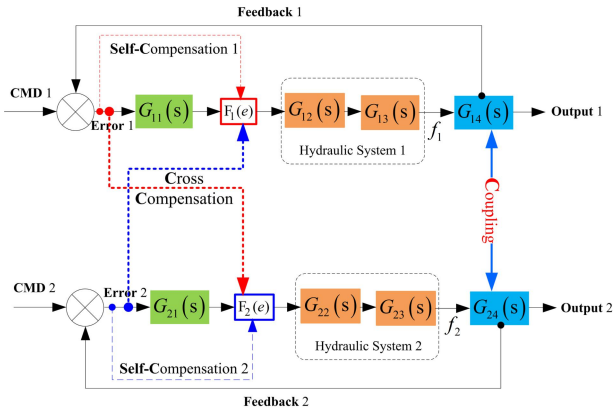

Fig. 4 Block diagram of two-channel closed-loop cross compensation controller

In Fig. 3, $G_{1k}(s)$ and $G_{2k}(s)$ (k=1, 2, 3, 4), are transfer function of test components respectively. And $F_1(e)$ and $F_2(e)$ are compensation function. In Figure 5, multi-channel cross coupling compensation control contains the cross compensation between channel 1 and channel 2. At the same time, it also includes self-compensation in the every control channel, as discussed in the SISO test system. Compensation function can be deduced using SCM between two channels.

To deduce SCM, a simple two-channel case of a cantilever is built, as Fig. 4 illustrated. In addition, this paper merely focuses on elastic deformation of cantilever, and ignores its plastic deformation.

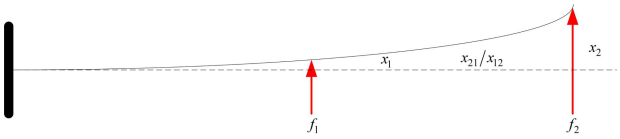

Fig. 5 Two-channel cantilever example

Fig 4 is described as Equation (16).

$$\begin{cases} f = K \cdot x \\ \begin{bmatrix} f_1 \\ f_2 \end{bmatrix} = \begin{bmatrix} K_{11} & K_{12} \\ K_{21} & K_{22} \end{bmatrix} \begin{bmatrix} x_1 \\ x_2 \end{bmatrix} \end{cases} \quad (16)$$

For analysis purposes, it is assumed that the SCM is invertible. Actually, it does not need to be inverted, as it is the terms of the compliance matrix, which are either measured or calculated, that are used in the implementation.

SCM can be described as Equation (17).

$$SCM_{2\times 2} = \begin{bmatrix} K_{11} & K_{12} \\ K_{21} & K_{22} \end{bmatrix} \quad (17)$$

Where, SCM is extended from 2 order to n order, as equation (18) shown.

$$SCM_{n\times n} = \begin{bmatrix} K_{11} & K_{12} & \cdots & K_{1n} \\ K_{21} & K_{22} & \cdots & K_{2n} \\ \vdots & \vdots & \ddots & \vdots \\ K_{n1} & K_{n2} & \cdots & K_{nn} \end{bmatrix} \quad (18)$$

In practice, SCM cannot describe the coupling mechanism exiting among the loading points fully, because the coupling effect yet contains other factors except stiffness coordinateness, such as location of loading points, loading setup and mechanical play. Theoretically, the cross coupling compensation factor matrix is obtained by SCM. And then Cross Compensation Matrix (CCM) is obtained. The cross compensation factor needs to be modified by manual tuning in the test implementation.

3.2 Methods of generating stiffness coordinate matrix

There are TWO methods of determining the stiffness coordinate matrix coefficients: by finite element modeling and calculation and by manual tuning.

Finite Element Analysis: if a finite element model (FEM) of the test article under test exists, then SCM can be extracted fairly easily. What is required is to determine the deflection at every location as a function of a unit force applied to one location at a time. This is a quite sizable matrix, for an N channel test, stiffness coordinate matrix has N squared terms, and this is built up from N load cases. If these channels which have no coupling effect are ignored, the order of SCM is not huge.

Manual Tuning: the manual tuning technique is fairly simple but tedious as it takes several iterations to converge on a suitable set of stiffness coordinate matrix coefficients. Initially each actuator channel is tuned one channel at a time in load control. Interaction tuning is carried out by applying a triangular or sine load-waveform disturbance to a single channel while all other channels are commanded either a static or zero load. The interaction coefficients are then adjusted to remove the interaction errors.

SCM between loading points is deduced using FEM of test rig in this paper. Then the cross coupling compensation factors calculated theoretically can be modified before the test by manual tuning.

3.3 Methods of calculating cross compensation matrix

After the stiffness coordinate matrix is obtained using finite element analysis, the cross compensation matrix need to be calculated and deduced.

Multi-channel control system is decoupled using SCM being diagonalized.

Assuming that the H is invertible, Equation (19) can be obtained..

$$H^{-1} \cdot SCM \cdot H = \Lambda \quad (19)$$

The cross coupling compensation factor matrix H is obtained, as Equation (20) shown.

$$H_{n\times n} = \begin{bmatrix} h_{11} & h_{12} & \cdots & h_{1n} \\ h_{21} & h_{22} & \cdots & h_{2n} \\ \vdots & \vdots & \ddots & \vdots \\ h_{n1} & h_{n2} & \cdots & h_{nn} \end{bmatrix} \quad (20)$$

In the multi-channel closed-loop compensation control, Equation (3) is rewritten as Equation (21).

$$F_{ij}(e_i) = \begin{cases} \left(1+h_{ij}\right) & (|e_i| \geq 1\%, i = j) \\ h_{ij}, (|e_i| \geq 1\%, i \neq j) \\ 1, (|e_i| < 0.5\%, i = j) \\ 0, (|e_i| < 0.5\%, i \neq j) \end{cases} \quad (21)$$

It is noted that the output signal of controller is compensated adaptively using new method.

CCM is calculated by Equation (20) and (21), as Equation (22) described.

$$CCM_{n\times n} = \begin{bmatrix} F_{11} & F_{12} & \cdots & F_{1n} \\ F_{21} & F_{22} & \cdots & F_{2n} \\ \vdots & \vdots & \ddots & \vdots \\ F_{n1} & F_{n2} & \cdots & F_{nn} \end{bmatrix} \quad (22)$$

Subsequently, CCM is introduced into a closed feedback control loop. And a cross compensation control algorithm was designed based on Equation (21).

Using that control algorithm, the output signal of every channel was compensated crossly and adaptively in the aim to decrease the coupling effect, control the loading system precisely, speed up the test system response, and reduce the test cost. The outputs signal ui of channel i was compensated crossly and adaptively shown as Equation (23).

$$u_i^{'} = u_1 F_{1i} + u_2 F_{2i} + \cdots + u_n F_{ni} \quad (22)$$

Where, ui' is output signal of channel i after compensated, ui'is output signal without compensation.

After U, as output signal of every controller, is compensated, U' is interpreted as Equation (24).

$$U^{'} = U \begin{bmatrix} F_{11} & F_{12} & \cdots & F_{1n} \\ F_{21} & F_{22} & \cdots & F_{2n} \\ \vdots & \vdots & \ddots & \vdots \\ F_{n1} & F_{n2} & \cdots & F_{nn} \end{bmatrix} \quad (23)$$

Where, U=[u1 ,u2, …un], U'=[u1' ,u2', …un']

It is easy to see that these channels containing less coupling effect cannot be considered. And this paper focus on strong coupling effect among channels, which is compensated to be decoupled using new method. If there is strong coupling among channel i, channel j and channel k, these channels need to be decoupled with no considering other channels, and then Equation (25) is obtained under in every channel.

$$\begin{cases} u_i^{'} = u_i F_{ii} + u_j F_{ji} + u_k F_{ki} \\ u_j^{'} = u_i F_{ij} + u_j F_{jj} + u_k F_{kj} \\ u_k^{'} = u_i F_{ik} + u_j F_{jk} + u_k F_{kk} \end{cases} \quad (26)$$

Obviously, the difficulty to partition compensation matrix in the literature [2] is solved using the new technology.

4 Application in fatigue testing system for wingbox structure

4.1 Test configuration

In order to validate the method in this paper, a Four-channel fatigue testing system for wingbox structure was designed, as Fig. 6 shown.

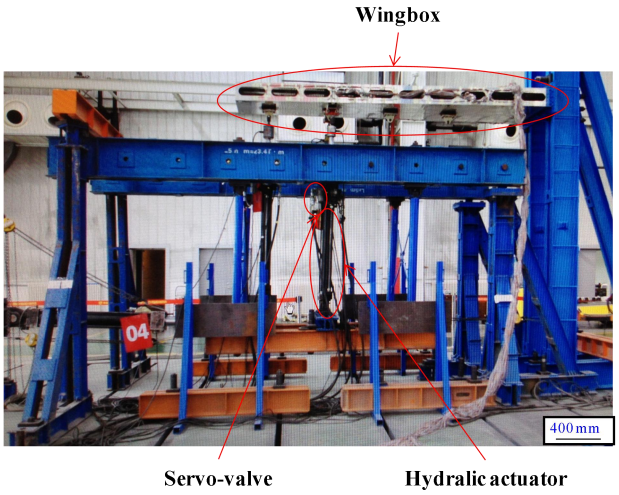

Fig. 6 Four-channel fatigue testing system for wingbox structure

The Wingbox Structural Fatigue Test has 4 channels of hydraulic load control. This method will be implemented using MTS AeroPro software and MTS Aero ST hardware.

4.2 Finite element modeling and calculation on test article

SCM is obtained mainly by finite element modeling and calculation in this paper. Owing to finite element model of the wingbox under test existing,

SCM can be extracted fairly easily. It is to determine the deflection at every location as a function of a unit force applied to one location at a time.

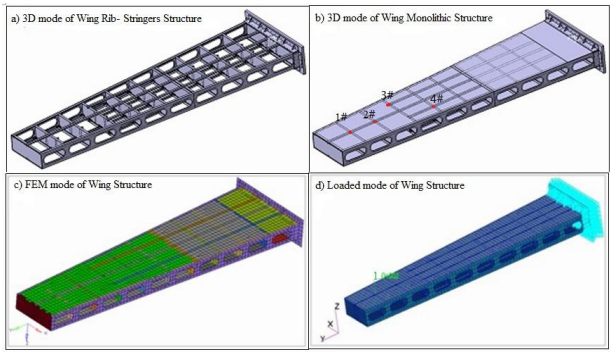

Fig. 7 Model of Wingbox structure, a) 3D mode of Wing Rib- Stringers Structure, b) 3D mode of Wing Monolithic Structure, c) FEM mode of Wingbox Structure, d) Loaded mode of Wingbox Structure.

The test article is designed as a wingbox structures, consist out of morphing, ten wing ribs, 3 stringers and 2 webs. The middle stringer perforates wingbox structure in span wise, as Fig. 7(a) shown. The morphing of wingbox structure is designed as a variable thickness structure in span wise. The thickness between rib 1 and rib 2 is 6 mm. The thickness between rib 2 and rib 5 is 4 mm. The thickness between rib 5 and rib 10 is 2 mm. The material of wingbox structure is aluminum. As for this material, Young's Modulus is 70 GPa，Poisson's Ratio is 0.346，Density is 2710 kg/m3, as Fig. 7(b) shown. The test setup of wingbox structure is demonstrated as Fig 5.

The FEM of wingbox structure is shown as Fig. 7(c). Then, Finite Element Analysis (FEA) is implemented for the wingbox structures. There are four loading points in the model. Loading point 1# is located on the intersection of rib 9 and middle stringer; Loading point 2# is located on the intersection of rib 8 and middle stringer; Loading point 3# is located on the intersection of rib 7 and 1st stringer; Loading point 4# is located on the intersection of rib 6 and 3st stringer, as Fig. 7(d) shown. SCM is calculated using FEA, as Equation (26) described.

$$SCM_{4\times4} = \begin{bmatrix} 323 & 393 & 484 & 618 \\ 390 & 435 & 534 & 674 \\ 480 & 534 & 569 & 766 \\ 614 & 674 & 766 & 776 \end{bmatrix} \quad (26)$$

Using Equation (26), the cross compensation factor matrix H is described as Equation (27).

$$H_{4\times4} = \begin{bmatrix} 0.4021 & 0.4533 & 0.6131 & 0.5116 \\ 0.4477 & 0.3532 & -0.7761 & 0.2618 \\ 0.5144 & 0.26170 & 0.1376 & -0.8043 \\ 0.6110 & -0.7754 & 0.0523 & 0.1512 \end{bmatrix} \quad (27)$$

As Equation (26) shown， the four loading points are interacted seriously. The cross compensation control is conducted among four channels using Equation (27). And H needs to be modified by manual tuning before fatigue test.

4.3 Control Law

The subset of control law in use on the Wingbox Structure Fatigue Test is AeroPro control. AeroPro now permits run-time calculated-inputs and calculated-outputs that can be programmed using an interpreted scripting language. These calculations are carried out at the system sample rate. This is the feature that is being used to implement multi-channel closed-loop cross coupling compensation control. The calculated-input and calculated-output scripts can access all other commands, feedback, error signals, stabilization inputs, analogue inputs, analogue outputs, virtual inputs, virtual outputs and system states from all other channels within an Aero ST console.

The calculations option allows users to change real-time signals (such as controller feedback), generate digital output and event-action logic, or manipulate the control law on a channel. Calculated virtual input and virtual output values are determined by applying a user-defined mathematical equation to the specified signal values.

Calculations execute in the real-time controller. Applying the calculations in the control loop allows

user to see an equation's results while a test is running instead of calculating them manually or waiting for post-test data analysis.

The calculated outputs is used to configure test control channels for complex drive functions for valves and other devices through D/A. During system configuration, each channel is built by assigning a control channel and an virtual channel. The control channel only contains signal output. And there are signal input and virtual signal output in the virtual channel. The calculated-output in the output signal of control channel can be programmed by virtual output signal to be assigned to the valve driver.

The compensation relationship described in Equation (28) is programmed to generate calculated-output script in the AeroPro control system to carry out closed-loop cross compensation in the AeroPro ST.

In the wingbox structural fatigue test system, the compensation factor is modified using manual tuning. The cross compensation factor matrix H is rewritten as Equation (28).

$$H_{4\times4}=\begin{bmatrix}0.6 & 0.3 & 0.8 & 0.9\\ 0.5 & 0.5 & -0.7 & 0.3\\ 0.8 & 0.4 & 0.4 & -0.8\\ 0.7 & -0.6 & 0.1 & 0.1\end{bmatrix} \tag{28}$$

When, in every channel U can be compensated, as Equation (29) described.

$$\begin{cases} u_1^{'} = 1.6u_1 + 0.5u_2 + 0.8u_3 + 0.7u_4 \\ u_2^{'} = 0.3u_1 + 1.5u_2 + 0.4u_3 - 0.6u_4 \\ u_3^{'} = 0.8u_1 - 0.7u_2 + 1.4u_3 + 0.1u_4 \\ u_4^{'} = 0.9u_1 + 0.3u_2 - 0.8u_3 + 1.1u_4 \end{cases} \tag{29}$$

When , U needs to be compensated.

Using cross compensation relationship shown as Equation (28).

5 Results and Discussions

The experiment results of channel 2 is described as Fig. 9. In this paper, the experiment data of channel 2 is given merely. And data of other 3 channels would not be discussed.

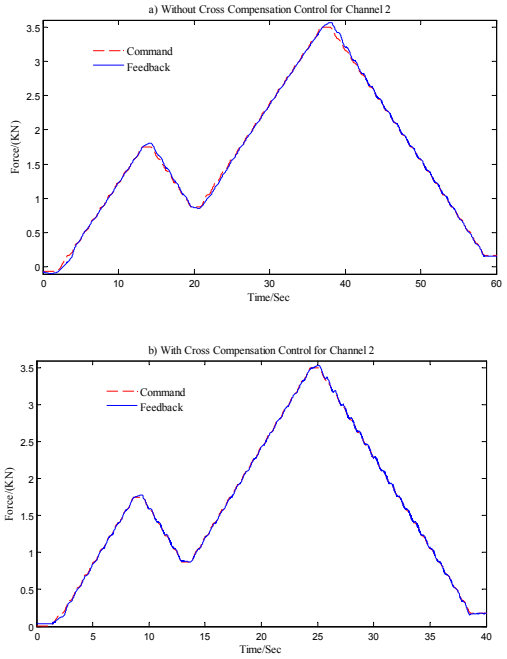

Fig. 8 Experimental data comparisons, (a) Without cross compensation control for Channel 2, (b) With cross compensation control for Channel 2.

There is some unnecessary vibration in the curve of feedback, as Fig. 8(a) shown. While the factor hij is inserted in channel 2, there is less vibration in the curve of feedback as Fig. 8(b) shown. Obviously, the compensation in control channel 2 is efficient.

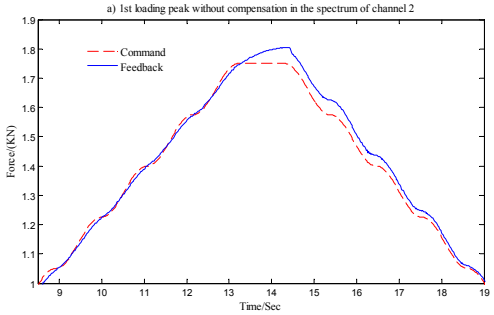

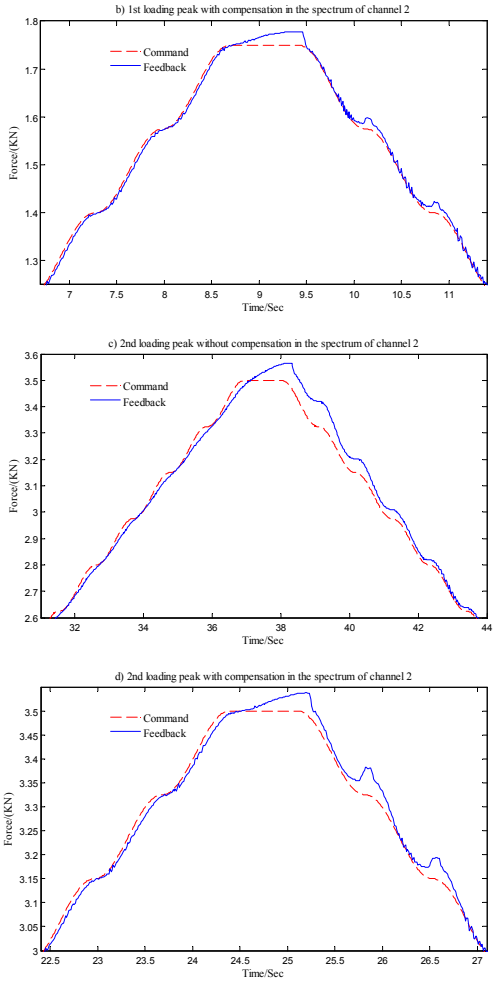

Fig. 9 Experimental data comparisons for two loading peak, a) 1st loading peak without compensation in the spectrum of channel 2; b) 1st loading peak with compensation in the spectrum of channel 2; c) 2nd loading peak without compensation in the spectrum of channel 2; d) 2nd loading peak with compensation in the spectrum of channel 2.

At the mean time, loading condition for two loading peak in the spectrum of channel 2 is analyzed and studied with no compensation and compensation, as Fig. 9(a, b, c, d) described. In 1st loading peak, load error is 2%, mean time to load is 9.5s, as Fig. 9a described; with compensation, load error is 0.3%, mean time to load is 5s, as Fig. 9b described. In 2nd loading peak, load error is 1.8%, mean time to load is 12s, as Fig. 9c described; with compensation, load error is 0.32%, mean time to load is 4.5s, as Fig. 9d described. Obviously, using cross compensation, control accuracy and loading speed were improved.

In other 3 control channels, with cross compensation control, fatigue testing system for wingbox structure is accelerated by 10~20 seconds. And the control accuracy of control channels is improved and stay near the 0.3%.

6 Conclusions

The control techniques outlined in this paper have been researching in various forms for a number of years. However, the implementations discussed are related particularly to the unique problems encountered in full-scale fatigue testing and have been proven to be effective on fatigue tests of the wingbox structure in this paper. The major benefit is the potential for faster testing without compromising control stability. For a test where there is a high level of interaction causing long settling times at load conditions, the benefits can be at least a 15% improvement in test running rate. This is significant test saving for a test program that involves several years of testing. Further major benefits are improved control stability due to linearization, improved static accuracy and improved repeatability. The flexibility of modem commercial control systems now permits these techniques to be implemented and customised for individual testing scenarios, without the cost and complexity of modifying critical run-time control system software.

References

[1] Yudi Ardianto et al, Test program for the A380 major fatigue test, ICAF2005. Hamburg, UK (2005)353-376.

[2] Jorge Cabrejas et al.. C-295 fuselage full-scale fatigue and damage tolerance tests, ICAF2005. Hamburg, UK (2005) 657-668.

[3] Hans-Jurgen Schmidt, Damage tolerance technology for current and future aircraft structure, ICAF2005, Hamburg, 2005: 1-42.

[4] Jorge G. Bakuckas et al, Destructive evaluation and

extended fatigue testing of retired aircraft fuselage structure, ICAF2005. Hamburg, UK (2005) 229-240.

[5] Michal Dziendzikowski, Krzysztof Dragan, Artur Kurnyta et al, Damage Size Estimation of the Aircraft Structure with Use of Embedded Sensor Network Generating ElasticWaves, Key Engineering Materials, 598(1) (2014) 57-62.

[6] R. Sepe, E. Armentani, G. Lamanna, F. Caputo, Fatigue Be haviour of Full Scale Flat Stiffened Aeronautic Panels, Key Engineering Materials, 627(9) (2015) 97-100.

[7] Alfonso Apicella, Enrico Armentani, Stefano Priore, Fatigue Analysis on a Full Scale Fuselage Panel, Key Engineering Materials, 385-387(9) (2008) 549- 552.

[8] N.Robler, C.Peters, O.Tusch, G.Hilfer, C.Herrmann, Concept of the new A320 fatigue test. ICAF2009, Rotterdam, (2009) 225-236.

[9] Rushabh Kothari, Full-Scale Static and Fatigue Testing of Composite Fuselage Section, ICAF2011, Montreal, (2011) 551-560.

[10] Felix Schwarberg and Frank Eichelbanm, An efficient load introduction concept for the A380 full-scale fatigue test, ICAF2005, Hamburg, UK (2005) 365-376.

[11] Andrzej Leski, Piotr Reymer, and Marcin Kurdelski, Development of Load Spectrum for Full Scale Fatigue Test of a Trainer Aircraft, ICAF2011, Montreal, (2011) 573-583.

[12] G. Hilfer, N. Rößler, C. Peters, and C. Herrmann, A320 ESG Full Scale Fatigue Test - Lessons Learned, ICAF2011, Montreal, (2011) 529-537.

[13] L. Molent, S.A. Barter, P. White, B. Dixon, Damage tolerance demonstration testing for the Australian FA-18, International Journal of Fatigue, 31(2009) 1031–1038.

[14] Yuval Freed1 and Sven Rzepka2, An Implementation of an Accelerated Testing Methodology to Obtain Static, Creep and Fatigue Master Curves of a T300913 Unidirectional Composite Material, ICAF2011, Montreal, (2011) 145-153.

[15] Yu Jiang, Gun Jin Yun, Li Zhao, Junyong Tao, Experimental Design and Validation of an Accelerated Random Vibration Fatigue Testing Methodology, 2015, http: // dx. doi. Org / 10. 1155/2015/147871.

[16] Dr. Andrew Halfpenny, Methods for Accelerating Dyanmic Durability Tests, 9th International Conference on Recent Advances in Structural Dynamics, Southampton, UK(2006) 341-356.

[17] J.Schijve, Load Sequences for Fatigue of Components and Full-scale Aircraft Structures, ICAS1970. Roma, (1970).

[18] Andrzej Leski, Piotr Reymer, and Marcin Kurdelski, Development of Load Spectrum for Full Scale Fatigue Test of a Trainer Aircraft, ICAF2011, Montreal, (2011) 573-583.

[19] Dale L. Ball, Philip C. Gross, Robert J. Burt, F-35 Full Scale Durability Modeling and Test, Advanced Materials Research., 891-892(3) (2014)693-701.

[20] Burnett G., Patterson A., Powlesland I., Morris P. and Roeloffi B., An Application of Parallel Processing to Distributed Real Time Control of Aircraft Testing, IEEE conference On Control Applications, IEEE, Glasgow, (1994) 817-824.

[21] Graeme Burnett, Scott Dutton, David Hartley and Michael Sullivan, Advanced control techniques for full-scale fatigue testing, ICAF2005, DGLR-Bericht, Hamburg, (2005) 481-492.

[22] N. C. Eenkhoorn. Development of Virtual Testing Methodology for Structural Fatigue Testing Setups, The Netherlands. Delft University of Technology, 2010.

Copyright Statement